Journal of Hydrology 617 (2023) 128891

Contents lists available at ScienceDirect

Journal of Hydrology

journal homepage: www.elsevier.com/locate/jhydrol

Research papers

Modeling groundwater transit time distributions and means across a Nebraska watershed: Effects of heterogeneity in the aquifer, riverbed, and recharge parameters

Caner Zeyrek [a], Aaron R. Mittelstet [b,*], Troy E. Gilmore [a,b], Vitaly Zlotnik [c], D. Kip Solomon [d], David P. Genereux [e], C. Eric Humphrey [d], Nawaraj Shrestha [a]

[a] Conservation and Survey Division – School of Natural Resources, University of Nebraska – Lincoln, USA
[b] Biological Systems Engineering Department, University of Nebraska – Lincoln, USA
[c] Department of Earth and Atmospheric Sciences, University of Nebraska – Lincoln, USA
[d] University of Utah, Department of Geology and Geophysics, USA
[e] North Carolina State University, Department of Marine, Earth, and Atmospheric Sciences, USA

ARTICLE INFO

Keywords:
Groundwater modeling
Particle tracking
Groundwater transit times
Nebraska Sand Hills

ABSTRACT

Groundwater transit time distributions (TTDs), the travel times through the aquifer from recharge at the water table to discharge at the surface water body, provide critical information on the timescales of hydrologic response of subsurface flow systems. We investigated the effects of spatial patterns of recharge, aquifer heterogeneity, and systematic variation in riverbed hydraulic conductivity on the mean transit times (MTTs) and TTDs of groundwater discharge to the Upper Middle Loup River (UMLR) and headwaters using a 3D-steady-state MODFLOW USG-MODPATHD3DU model. This 5436 km^2 watershed overlies the High Plains Aquifer in the Sand Hills of Nebraska, USA. Modeled MTTs differed by up to three orders of magnitude from upstream to downstream in a 158 km section of the UMLR under varying recharge, aquifer, and riverbed heterogeneity scenarios. The simulated MTTs ranged from 1 to 397 years for upstream sites and 820 to 7968 years for the downstream sites. The TTDs at upstream sites were dominated by young groundwater from shallow flow paths and were sensitive to changes in riverbed hydraulic conductivity. Recharge parameterization had greater influence on the shape of the TTDs and magnitude of MTTs at the downstream sites, where much older groundwater discharged to the UMLR. Overall, spatial trends in transit times under varying model scenarios provided important information for refined conceptualization and calibration of future numerical models.

1. Introduction

Modeling groundwater mean transit times (MTTs) and transit time distributions (TTDs) is critical for characterizing the hydrological responses of subsurface flow systems (Jing et al., 2019) and estimating travel times for contaminants that discharge from aquifers (Basu et al., 2012; Ilampooranan et al., 2019; Leray et al., 2019; Browne and Guldan 2005; Modica et al., 1998; Kennedy et al. 2009; Gilmore et al., 2016). Groundwater TTDs are especially effective tools for evaluating lag times between the input of non-point-source pollution and its discharge to groundwater wells and streams. Different analytical lumped-parameter models (LPMs) and coupled numerical groundwater models and particle tracking algorithms can be used to simulate groundwater TTDs. Lumped parameter models are characterized by the TTD functions whose parameters can be calibrated by the experimental observations of tracers transported between recharge (input) and discharge (output) areas (Małoszewski and Zuber, 1982; Maloszewski, 2000). Numerical groundwater and transport models are mainly based on the solution of the groundwater flow and transport equations in which the transit times could be governed by advection-only conditions (i.e., kinematic age, Modica et al., 1998; Maxwell et al., 2016; Eberts et al, 2012; Basu et al., 2012; Gusyev et al., 2014) or advection along with other transport processes such as dispersion, diffusion and reaction (Goode, 1996; Varni and Carrera, 1998). The latter is based on equations derived from both residence-time-distribution concepts and mass-conservation principles applied to conceptual age mass rather than just kinematic ages based on

* Corresponding author.
E-mail address: amittelstet2@unl.edu (A.R. Mittelstet).

https://doi.org/10.1016/j.jhydrol.2022.128891
Received 15 July 2022; Received in revised form 10 November 2022; Accepted 23 November 2022
Available online 13 December 2022

average linear groundwater velocities.

The effects of spatially varying recharge or aquifer hydraulic parameters on the shape of TTDs have been investigated in multiple studies (Abrams and Haitjema, 2018; Jing et al., 2019; Leray et al., 2019; Rumynin et al., 2019; Sanford 2011; Edington and Poeter, 2006). The effects of heterogeneity in riverbed conductivity on fluxes between aquifer and river have been studied (e.g., Irvine et al., 2012; Kurtz et al., 2013; Tang et al., 2017), however effects of riverbed hydraulic conductivity on the groundwater TTDs have not been explored. Engdahl and Maxwell (2015) studied the effects of recharge variation induced by climate change on TTDs which had significant changes between different climate scenarios. Abrams and Haitjema (2018) simulated TTDs using an LPM and MODFLOW-MODPATH and concluded that the parameters such as saturated thickness, porosity and groundwater recharge control the shape of the exponential TTDs. A catchment-scale groundwater TTD study carried out by Jing et al. (2019) showed that the shape of TTDs is strongly dependent on groundwater recharge rates and sensitive to recharge spatial patterns. Effects of non-uniform aquifer structure and groundwater recharge conditions on residence time distributions were investigated by Leray et al. (2019) using an analytical modeling approach. Their study found that the shape of the residence time distribution is significantly modified by including the aquifer structure and recharge gradients in their semi-analytical model. Etcheverry and Perrochet (2000) linked the asymmetry and multimodality in the TTDs to the aquifer geometry and heterogeneity in the groundwater flow velocities where they modeled a regional multilayered aquifer using an analytical method.

Understanding the vertical variations in hydraulic properties of aquifers is critical for explaining the groundwater flow dynamics (Dietze and Dietrich, 2012). An increase of hydraulic conductivity with depth in some stratigraphic sequences results from depositional processes in sand-bed braided rivers (Zlotnik et al., 2011). On the contrary, a decrease of hydraulic conductivity with depth in consolidated systems is generally attributed to spatial variation in fracture intensity where the fractures in the shallow crust deformed in response to stresses induced by earthquake waves, earth tides, tectonic stresses and groundwater pumping (Earnest and Boutt, 2014) and also compaction due to the greater total stress (Fetter, 2001, p. 89).

Cardenas and Jiang (2010) state that the exponentially decreasing regional scale heterogeneity enhances the power law residence time distribution by increasing the deeper slow flowing zone and accelerating the fluxes near the land surface. Furthermore, Rumynin et al. (2019) investigated the effects of hydraulic conductivity anisotropy and depth-decay coefficients on groundwater flow and TTDs using computational simulations. They concluded that the relationship between TTDs and the monotonically increasing and decreasing hydraulic conductivity may exhibit non-monotonic behavior. Edington and Poeter (2006) investigated the effects of vertical heterogeneity on travel times using a MODFLOW-MODPATH model where they obtained the geological model using a stratigraphy simulator, FLUVSIM. Their study concluded that groundwater travel times were younger under a low-accommodation (e.g., low amount of space available for sediment accumulation) stratigraphy and older under high-accommodation stratigraphy. Sanford (2011) also found that the spatial variation in recharge and hydraulic conductivity makes a significant difference in age distributions, but the sensitivity of age to vertical hydraulic conductivity is not clear since it is generally poorly constrained in modeling studies.

Past theoretical studies indicate that simulated transit times are sensitive to spatial heterogeneity in recharge, aquifer structure, and likely, streambed conductance. However, there is lack of site-specific studies that systematically account for the effect of heterogeneity of these parameters on groundwater TTD modeled for multiple streambed discharge points at a watershed scale. The objective of our study was to evaluate the effects of spatial complexity of recharge, structural heterogeneity of aquifer characteristics, and systematic variation in riverbed hydraulic conductivity on the TTDs and MTTs in six river sites along a 158 km section of the Upper Middle Loup River (UMLR) in the Nebraska Sand Hills. This study yields insight into model sensitivity of TTDs, at different spatial scales (ranging between 14 and 5436 km^2), that can aid future groundwater studies.

2. Methods

Modeling code MODFLOW-USG (Panday et al., 2012) was used to simulate three-dimensional steady-state groundwater flow in the Upper Middle Loup River (UMLR) watershed (Fig. 1). After a base model scenario (uniform recharge, aquifer and streambed parameters, Fig. 1, Step 3A), hypothetical recharge and aquifer parameter scenarios were applied in the model (Fig. 1, Steps 3B and 3C, respectively). Finally, the role of the magnitude and heterogeneity of riverbed conductance was investigated (Fig. 1, Step D). For each scenario, groundwater TTDs from backward particle tracking were examined (Step 4 through Step 6) to determine the effect of the different recharge and hydrogeologic heterogeneity scenarios on TTDs at aquifer discharge points (i.e., six study sites, Fig. 1).

Particle tracking was accomplished using MODPATH3DU code (Muffels et al., 2016). Unstructured grid discretization was chosen to increase the model performance and the computational efficiency by refining only river cells in the flow domain. MODPATH3DU was selected as a particle tracking code since it can handle high spatial variability of flow fields in the individual unstructured cells, where the particle tracking scheme is not susceptible to weak sinks (Craig et al., 2020).

2.1. Study site

This study focuses on systematic evaluation of hydrologic processes that potentially control the characteristics of groundwater TTDs of groundwater discharging to the UMLR. The UMLR watershed, which covers an area of 5436 km^2 in the Nebraska Sand Hills, drains to the United States Geological Station (USGS) stream gage station 06775500 (Fig. 2).

The Sand Hills are composed of vegetated sand dunes. Radiocarbon studies indicate dune mobility at various times during the Holocene epoch (Schmeisser McKean et al., 2015; Loope and Swinehart 2000). Most of the Sand Hills are used for grazing cattle with pasture making up 94 % of the study area Dappen et al. (2007). Average annual temperature is 10 °C and there is a large precipitation gradient from west to east (400 mm to 700 mm, respectively) across the Sand Hills with a mean annual precipitation and groundwater recharge of 533 mm and 73 mm, respectively (Szilagyi and Jozsa, 2013).

The aquifer in the study area is part of the northern High Plains aquifer composed of one or more hydraulically connected geological units of Quaternary and late Tertiary age (Gutentag et al., 1984). The uppermost geological unit in the Sand Hills is the Holocene eolian dunes and Pleistocene sand, gravel, silt and clay which overlies the Pliocene sands and gravels (Korus et al., 2011). Sand and sandstone of Miocene and Oligocene units (Ogallala Group) comprise the major aquifer unit in the Sand Hills (Korus et al., 2011). The base of the aquifer system is the siltstones of the Miocene Ogallala and Oligocene Arikaree groups. Saturated aquifer thickness varies from near zero to 314 m with an average of 161 m (Rossman et al., 2018). There are very few artificial aquifer stresses such as pumping to cause transient groundwater flow conditions as cropland makes up only 0.23 % of the model area and population is sparse.

The stream discharge in the Sand Hills is stable, with ratio of low- to high-flow (Q95/Q5) of only 1.41 with a Q95 of 16.3 m^3s^{-1} and Q5 of 11.5 m^3s^{-1} (Hobza and Schepers, 2018). Q95 and Q5 are the flow in m^3s^{-1} which was equaled or exceeded for 95 % and 5 % of the flow record, respectively. Riverbed hydraulic conductivity (K) varies significantly throughout the study area. Humphrey et al. (2020) measured riverbed K using arrays and/or transects of tube seepage meters

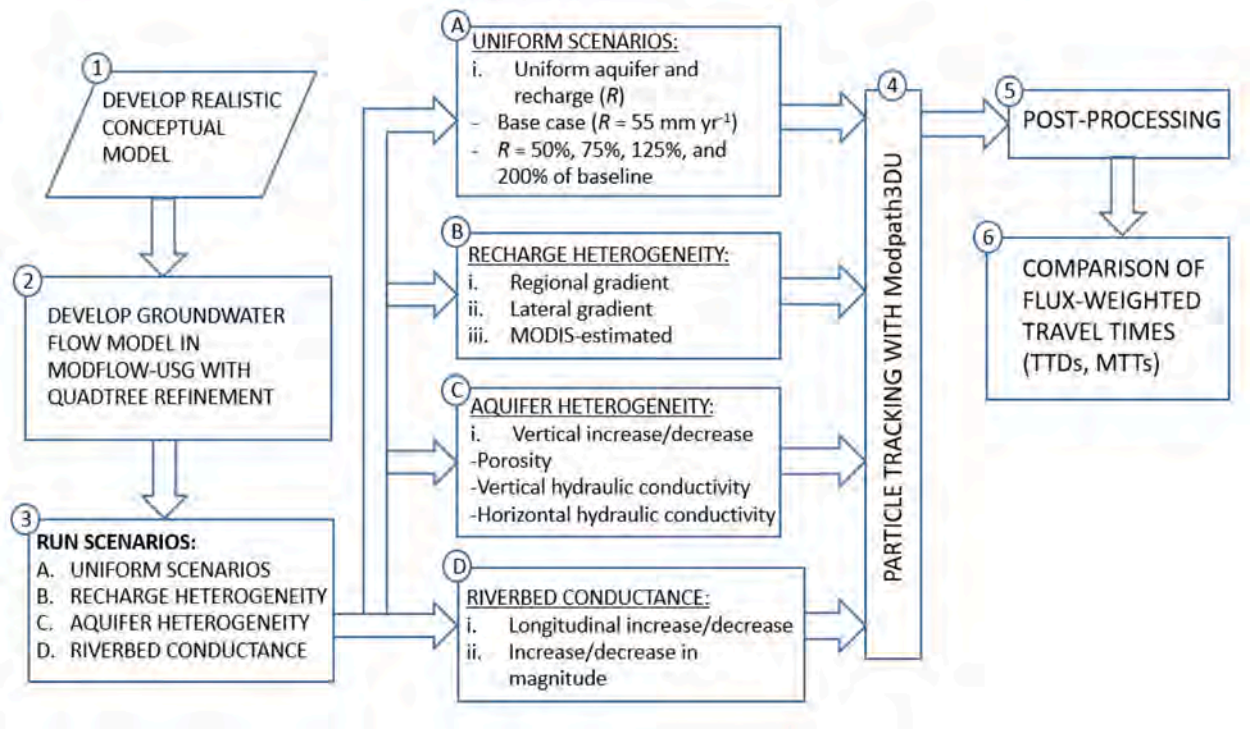

Fig. 1. Flow chart of the modeling approach. Steps 1–6 show the different processes starting from conceptual model development to estimating the mean transit times and transit time distributions. Varying recharge, aquifer and riverbed conductivity scenarios are also shown in the boxes from A to D in Step 3.

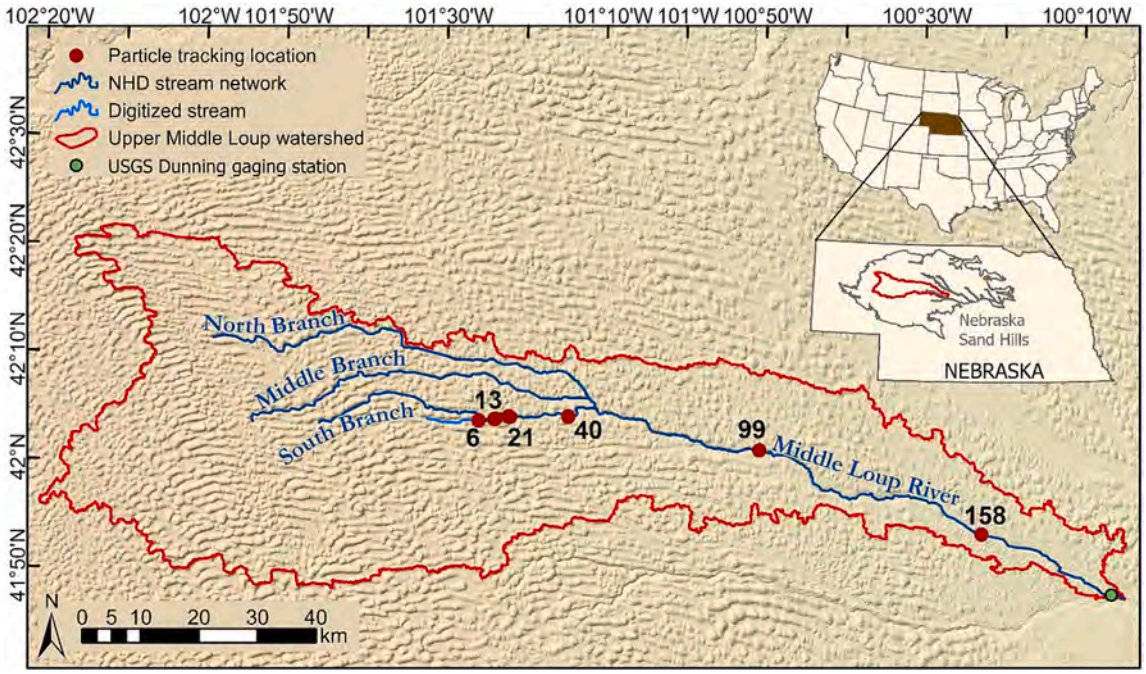

Fig. 2. Location map of the Upper Middle Loup River watershed. Each particle tracking site is labeled by its distance downriver, in km, from an arbitrary zero point, a culvert in the channel at Gudmundsen Research Laboratory. Inset in top right illustrates the location of the study site is within the Nebraska Sand Hills and the United States. The background map is created using LIDAR dataset with a 500 m resolution (USGS, 2022).

(Solomon et al. 2020) in six streambed sampling sites (2 km, 6 km, 13 km, 21 km, 40 km, and 99 km sites; Fig. 2). The average riverbed K values for the six sampling sites were 0.09 m/d, 3.94 m/d, 7.04 m/d, 8.89 m/d, 6.00 m/d and 15.74 m/d, from 2 to 99 km, respectively. Each study site is named by its distance downriver, in km, from an arbitrary zero point, a culvert in the channel at Gudmundsen Sandhills Laboratory (Gudmundsen Sandhills Laboratory | Nebraska Extension [WWW Document], n.d.).

2.2. Numerical groundwater flow model

Groundwater flow model code, MODFLOW-USG, coupled with the

Groundwater Vistas 7 (Rumbaugh and Rumbaugh, 2017) graphical user interface (GUI) was used to simulate three-dimensional steady-state flow. This code uses a finite difference numerical approximation method to solve the governing partial differential flow equation in a discretized flow domain.

The area of the flow domain was determined as 5436 km^2 based on the physical boundary conditions of the aquifer system within the watershed. The base of the aquifer was set as a no-flow boundary which represents the low hydraulic conductivity siltstone and claystone levels of the Oligocene age White River Group. We used the base of the aquifer contour map, which was developed using available borehole datasets (Conservation and Survey Division of University of Nebraska-Lincoln, 2019a). A 10 m digital elevation model (DEM) was used to represent the top surface of the model domain (USGS, 2017). Western, southern, and northern boundaries were chosen as no-flow boundaries which follow the groundwater divides across the flow domain based on a regional groundwater table map (Conservation and Survey Division of University of Nebraska-Lincoln, 2019b). A constant head boundary was assigned to represent the eastern model boundary based on the potentiometric head contours of the same regional groundwater table map.

An unstructured (Quadtree) grid refinement (Panday et al., 2013) was used for horizontal discretization of the model domain to create finer grids over and in the vicinity of the streams. The Quadtree grids formed only 5 % of the entire numerical model with two different grid sizes of 250 m and 125 m while the parent grid size remained 500 m. Aquifer thickness was divided into five layers to simulate the particle streamlines within the three-dimensional flow domain. Model layers were assigned as unconfined where the transmissivity is calculated from the saturated thickness and horizontal hydraulic conductivity of the model layer. Since long-term groundwater levels and discharge show very little variation (Rossman et al., 2018), a steady-state simulation was used.

2.3. Particle tracking simulations

The 5-layer regional groundwater flow model was developed to run the particle tracking simulations under steady-state conditions. A particle tracking code calculates the velocities and tracks the movement of imaginary particles using modeled head distribution, hydraulic conductivity, and effective porosity (Anderson et al., 2015). These particles travel with the average linear groundwater velocity (Darcy flux divided by effective porosity) which represents the advective transport of the solutes. The principal components of the velocity vectors in the model cells are calculated with an interpolation method and then the particle streamlines are traced using a particle movement technique. Derivations of the related particle tracking equations can be found in Muffels et al., 2016.

The lag time effect of the unsaturated zone (see Szilagyi et al., 2011; Szilagyi et al., 2003) on the TTDs was neglected throughout the simulations since the particle tracking clock starts at the potentiometric surface of the aquifer. Travel times for each numerical model scenario were simulated using a backward particle tracking scheme. Equal numbers of hypothetical particles located on the river boundary grids representing the different sampling sites were traced backward to their initial recharge locations.

MODPATH 3DU output files containing the particle travel times and streamlines obtained from each scenario were then post-processed in ArcGIS and coding environments. The flux-weighted TTDs for each streambed sampling site was represented by the recharge-weighted Cumulative Frequency Distribution (CFRD) of the transit times and the weighted-MTTs were calculated using the following equation (Kennedy et al. 2009; Gilmore et al. 2016):

$$MTT = \frac{\sum_{i=1}^{n} r_i t_i}{\sum_{i=1}^{n} r_i} \quad (1)$$

where, n is the total number of particles, t_i(T) is the particle transit time and r_i (L/T) is the recharge flux at the cell where the particle originates.

An MTT based on the exponential LPM was also calculated for comparison with the numerical MTTs using the following Eq. (2) derived by Haitjema (1995):

$$\mathrm{MTT} = \frac{nH}{N} \quad (2)$$

where n is the uniform porosity, N (L/T) is the uniform recharge and H (L) is the average saturated aquifer thickness which is assumed to be constant. The nH term represents the volume of the groundwater per unit area of aquifer (L^3/L^2) and N is the volumetric replenishment of groundwater into the aquifer per unit area of aquifer (L^3/L^2T). Since both H and N are expressed per unit area ($1/L^2$), an exact domain surface area is not required to calculate MTT.

2.4. Modeling scenarios

2.4.1. Baseline scenario

The baseline numerical model was run under uniform recharge and aquifer parameterization. An average recharge value of 55 mm yr^{-1} was obtained from MODIS-derived net groundwater recharge map (Szilagyi and Jozsa, 2013) and applied to the uppermost active layer in the model domain. Hydraulic conductivity used average value from Houston et al. (2013), which used a thickness-weighted average of the dataset of hydraulic conductivity and specific yield for the entire High Plains Aquifer. Calculated average uniform horizontal hydraulic conductivity (K_x) of 11 m/d was assigned to all active model cells. Vertical hydraulic conductivity (K_z) was assumed to be uniform and 1.1 md^{-1} (0.1 of the K_x). A vertical anisotropy ratio of 0.1 was considered to be conservative for the purpose of the modeling based on the physical characteristics of the unconsolidated and bedrock aquifers. The anisotropy ratios for the similar units were generally reported in the range of 0.01 and 0.5 (Domenico and Schwartz, 1990; Todd and Mays, 2005).

An average uniform porosity of 0.3 was chosen given the nature of the heterogeneous aquifer materials consisting of Plio-Quaternary and Pleistocene aged fine to medium sands and Miocene aged, consolidated sandstones (Fetter, 2001, p. 79).

A uniform riverbed hydraulic conductivity value of 0.5 m d^{-1} (within the range of field measurements) was chosen to get a better match between simulated heads and regional groundwater table counter map of the study area. The model setup for baseline groundwater flow model and particle tracking simulation scenario is given in Table S1.

2.4.2. Recharge heterogeneity scenarios

Uniform and spatially varying recharge conditions were considered. Uniform recharge scenarios were chosen as 50 %, 75 %, 125 % and 200 % of baseline recharge of 55 mm y^{-1}. Four different scenarios of spatial variability were simulated: general west-to-east gradient with increasing and decreasing patterns; a lateral gradient, where recharge is lower near the stream due to higher evapotranspiration; and MODIS-based distributed net recharge model. In each scenario, aquifer and river properties remained identical. Also, each spatially varying recharge scenario used the same total recharge as the baseline scenario (55 mm yr^{-1}).

In the first two scenarios with spatially varying recharge, the model domain was divided into five equal areas with different recharge rates (Fig. 3A). In scenario 1 recharge increased from west to east, and in scenario 2 recharge decreased from west to east. Calculated recharge values for the zones varied from 27.4 mm yr^{-1} to 82.1 mm yr^{-1}.

The third scenario was based on a lateral gradient along the channel, where recharge was lower near the stream due to higher evapotranspiration. Lateral extent of the stream buffers was determined based on analysis of the Normalized Difference Vegetation Index (NDVI) for the study site (Fig. 3B). NDVI is an index based on the reflectance

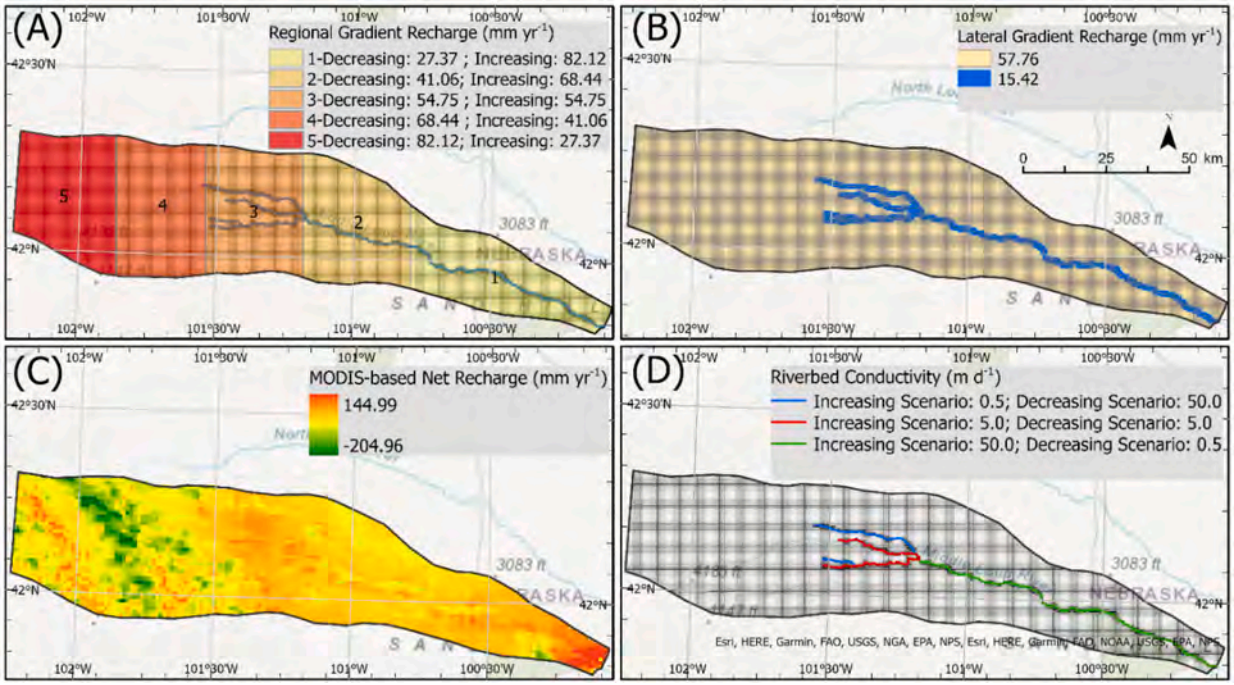

Fig. 3. Variation in model parameters, including distribution of groundwater recharge for (A) east to west gradient scenarios, (B) NDVI-based lateral recharge gradient scenario and (C) MODIS-based model scenario, and (D) stream segments and conductance values used in the varying riverbed conductance simulations.

measurements in the visible and near-infrared regions of the spectra to examine the dynamics of vegetation (Deering, 1978).

In arid and semi-arid regions, groundwater is a critical source for plant growth and transpiration (Naumburg et al., 2005; Wang et al., 2011; Seeyan et al., 2014). Thus, this may lead to a reduction in young groundwater discharging to streams. A recent study (Parizi et al. 2020) concluded that when NDVI was >0.18, groundwater recharge started decreasing with increasing NDVI in their semi-arid study area. Given the similar climatic conditions and high mean NDVI (<0.32) in our study area, we used this assumption in the lateral gradient recharge scenario.

Multispectral satellite images (from Landsat TM/OLI) were used to calculate the NDVI:

$$\mathrm{NDVI} = \frac{\mathrm{NIR} - \mathrm{RED}}{\mathrm{NIR} + RED} \tag{3}$$

where NIR is the reflection in the near-infrared spectrum and RED is the reflection in the red ranges of the spectrum.

The red and near-infrared bands of Landsat-8 surface reflectance images were used to calculate the NDVI (Myneni et al., 1995) in Google Earth engine. The satellite images were cloud masked using pixel quality values (Vermote et al., 2016) and were filtered for cloud cover <5 %. To represent the growing season, average NDVI between May and July were calculated from 2013 to 2020. The NDVI values were then aggregated within the river and non-river boundary condition cells. The numerical model cells within the stream buffer zones were assigned the highest average NDVI values while the cells outside the stream were given the lowest average NDVI values. The total volume of recharge (8.15×10^5 m^3 d^{-1}) was then divided into river and non-river boundary cells based on the NDVI ratio. Recharge values for the stream buffer zones and the rest of the model domain cells were calculated as 15.42 mm yr^{-1} and 57.76 mm yr^{-1}, respectively (Fig. 3B).

The fourth recharge scenario used MODIS-derived distributed net groundwater recharge data with a 1 km resolution (Szilagyi and Jozsa, 2013) (Fig. 3C). Calculated recharge ranged between 140 mm yr^{-1} and −170.00 mm yr^{-1}. The minimum recharge occurred in the western part of the study area where there are multiple lakes and wetlands, and evapotranspiration exceeds precipitation.

2.4.3. Aquifer heterogeneity scenarios

Effects of regional scale aquifer heterogeneity on the TTDs were investigated using six hypothetical aquifer scenarios, where porosity and horizontal and vertical hydraulic conductivity values increased (three scenarios) or decreased (three scenarios) with the model layer numbers (Table S2). For increase and decrease scenarios, parameter values for five different layers were assigned in increasing and decreasing order. In the case of increasing porosity, for example, the shallowest layer (Layer 1) was set to 0.1, with increasing porosity values for each layer up to 0.5 for the deepest layer (Layer 5) (Table S2). Porosity range used in the aquifer heterogeneity scenarios was determined based on the wide range of consolidated and unconsolidated lithological units (unconsolidated sand, gravel, silt, clay, and sandstone). In scenarios with varying horizontal hydraulic conductivity, an anisotropy ratio (K_z/K_h) of 0.1 was used for all layers. Horizontal hydraulic conductivity was 11 m/d in vertical hydraulic conductivity scenarios. Hydraulic conductivity range was chosen based on a calibrated hydraulic conductivity distribution map (Rossman et al., 2018) for the study area. Since the modeled heads are less sensitive to a change in vertical hydraulic conductivity of the model layers than to a change in horizontal conductivity, a greater order of change in Kz was preferred.

2.4.4. River conductance scenarios

Riverbed hydraulic conductivity was simulated by assigning i) uniform riverbed conductivity values (0.05, 0.5, 5, 50 m/d) and ii) increasing or decreasing riverbed conductivity values from west to east (Fig. 3D). Riverbed conductivities were chosen within the range of values measured by Humphrey et al. (2020).

Interaction of groundwater and river was simulated by 'the river package', which is a head dependent-flux boundary (Harbaugh, 2005). Riverbed conductance (*CRIV*) relates the flux between the river and the aquifer to the head difference between aquifer and the river stage at a given river cell (Eq. (4)):

$$QRIV = CRIV(HRIV - h) \tag{4}$$

where *QRIV* is the flux between the aquifer and the river (L^3T^{-1}), *HRIV* is the river stage (L), *CRIV* is the riverbed hydraulic conductance (L^2T^{-1}),

and h is the head in the cell below the river reach (L). The riverbed hydraulic conductance can be calculated as follows:

$$CRIV = \frac{(KLW)}{M} \quad (5)$$

where L is the length of the river reach (L), W is the width of the river reach (L), M is the thickness of the riverbed (L), and K is the hydraulic conductivity of the riverbed material (LT^{-1}).

2.4.5. Statistical analysis of simulation results

The shapes of TTDs, obtained from different recharge, aquifer, and riverbed heterogeneity scenarios, were compared using descriptive statistics including higher moments of distributions and non-parametric Kolmogorov-Smirnov statistical test (KS) (Chakravarti et al., 1967). The KS test can be used to calculate the maximum absolute difference between two cumulative distributions, D_n at different significance levels (e.g. 0.05 or 0.01) as follows:

$$D_n = \max|M_1(X) - M_2(X)| \quad (6)$$

where $M_1(X)$ and $M_2(X)$ are two empirical distributions of random variable X. Also, D_n is between 0 and 1 and approaches 0 when two cumulative distributions get closer to each other.

3. Results and discussion

3.1. Baseline model scenario

Simulated water levels for the uncalibrated groundwater flow model scenario were generally in good agreement with regional groundwater table contours (Conservation and Survey Division of University of Nebraska-Lincoln, 2019b) except the western part of the model domain where hundreds of small wetlands and lakes reside (Fig. 4). This might be explained using uniform recharge in the baseline model, which does not represent the actual recharge distribution in these areas. Recharge is minimal or negative in the western portion of the model domain (Fig. 3C). Also, the spatial variations in the aquifer parameters control the head distributions throughout the flow domain. Saturated aquifer thickness obtained from the baseline model scenario varied between 150.5 m and 312.9 m with a mean of 227.2 m throughout the model domain.

The simulated transit times increased from upstream to downstream. The particle tracking sites in the stream ranged from 0.1 to 10,581 years (Table S3). Based on length of streamlines (Fig. 4) and corresponding transit times (Table S3), particles discharging at upstream sites (6 km, 13 km and 21 km), intermediate site (40 km) and downstream sites (99 km and 158 km) can be characterized by local, intermediate and deeper (regional) flow systems, respectively. In the upstream particle tracking sites at 6, 13, and 21 km, similar shallow particle streamlines, and distributions were observed, and transit times ranged from 0.1 to 2.9 years. Small transit times might be a result of the short local flow paths to the streams (Haitjema 1995). The intermediate particle tracking site of 40 km had transit times ranging from 0.1 to 150 years with a bimodal distribution (Fig. 5). The highest coefficient of variation (CV) of 101.91 % was also observed at this particle tracking site.

The longest transit times were observed at the downstream particle sites of 99 km and 158 km study sites which are located downstream of the confluence of the Upper, Middle, and Northern branches of the UMLR. Transit times ranged from 203 to 607 years and 2265 and 10582 years for 99 km and 158 km, respectively. Particles at the furthest downstream site of 158 km had a long-tailed TTD with relatively higher positive skewness due to the fewer old groundwater particles traveling through longer and deeper flow paths. Furthermore, moving from upstream to downstream, the shape of the TTDs gets closer to an exponential distribution which also may indicate that the furthest downstream discharge point receives groundwater from relatively larger portions of the aquifer in the model domain (Gusyev et al., 2014). Calculated analytical MTT of 1245 years (from Equation (2)) also suggests that numerical MTT is getting closer to an exponential MTT from upstream to downstream sampling points in the watershed (Haitjema 1995).

3.2. Recharge, aquifer and riverbed heterogeneity scenarios

Particle tracking simulation nomenclature for recharge, aquifer, and riverbed heterogeneity scenarios is provided in Table 2. Including the base case scenario, and considering six stream sites, the modeling effort yielded 120 different MTTs and TTDs. The related transit time statistics calculated for each parameter scenario are shown in Tables S3-S8 and Fig. S9. In the following sections we focus specifically on the MTTs and TTDs from the recharge, aquifer, and riverbed heterogeneity scenarios that yielded the greatest deviation from the baseline scenario (Fig. 6 and Table S8) to highlight important model parameters to consider in future

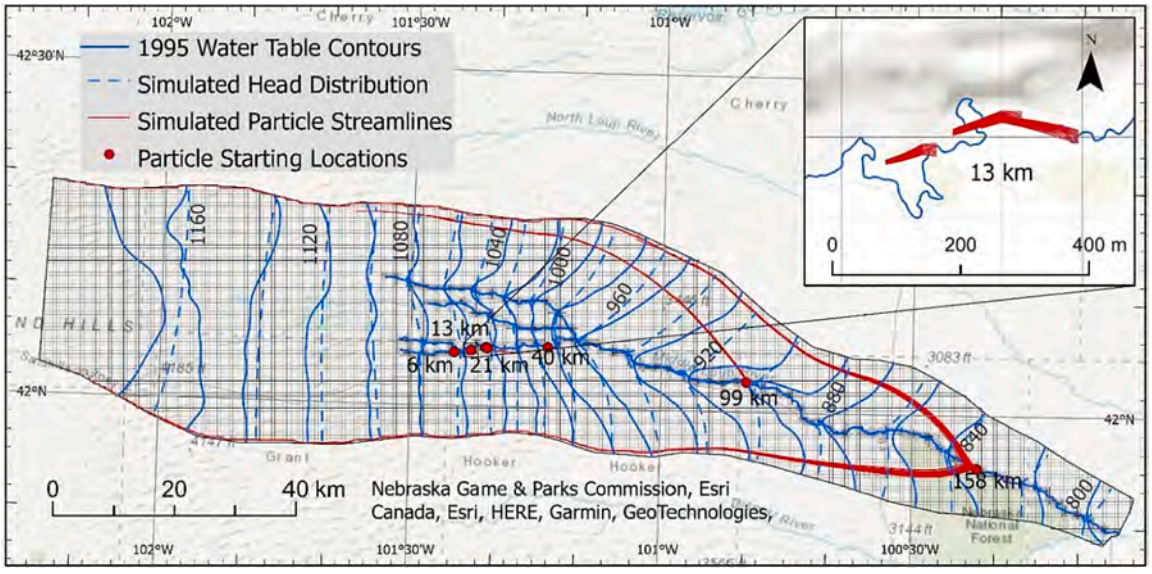

Fig. 4. Simulated steady-state head distribution, 1995 measured water table contours, and particle tracking streamlines for each study site for the baseline scenario. Short streamlines at 13 km site are also shown.

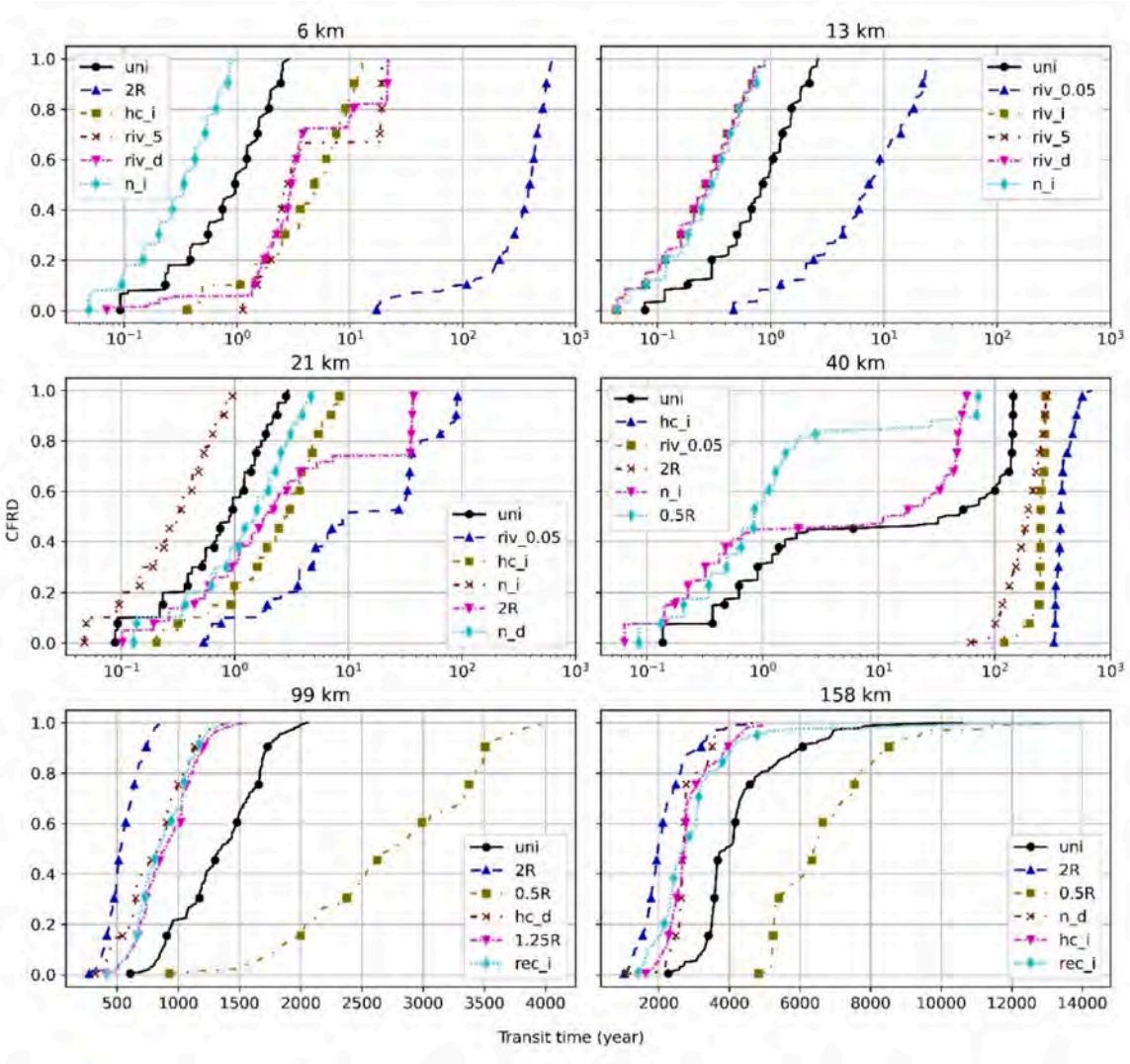

Fig. 5. The flux-weighted cumulative frequency distribution function (CFRD, i.e., the transit time distribution) curves for the baseline model scenario ("uni") and the five simulations with the highest Kolmogorov-Smirnov (KS) test scores for each of the six study sites shown in Fig. 2. Note that the horizontal axis for the 99 km and 158 km stream sites are plotted on a linear scale with different transit time ranges, while 6 km through 40 km sites are plotted on log scale with a consistent transit time range. The nomenclature is provided in Table 2.

particle tracking studies in similar hydrogeologic and climatic environments.

The sensitivity of the TTD to each scenario was evaluated based on the deviation from the TTD of the baseline scenario. The level of variation between the TTD of each scenario and the baseline scenario was quantified by maximum distance, D_n test score which was obtained from a two sample Kolmogorov-Smirnov test calculated at a significance level of 0.05 (Fig. 6 and Table S8). The calculated D_n scores varied from 0 and 1 where scores closer to 0 indicates a better match between two TTD distributions. The TTD curve of the scenarios which significantly (D_n test score >0.5 in Fig. 6) caused a shift from the baseline scenario were plotted for each study site (Fig. 5) and discussed in the following section.

A wide range of groundwater transit times was observed across the model domain with an increase in MTT from upstream to downstream under each scenario (e.g., Fig. 5, see also Fig. S9 and Table S3-S7). Upstream particle tracking sites at 6 km, 13 km and 21 km were dominated by local flow paths with short transit times. Intermediate and deeper flow paths resulted in longer transit times at 40 km, 99 km and 158 km. In general, transit times were more sensitive to a variation in riverbed hydraulic conductivity at upstream study sites (mean D_n of 0.42 and 0.29 for upstream and downstream, respectively; Table S8 and Fig. 6). Uniform recharge scenarios had the most influence on the shape of the TTDs in the downstream sites (mean D_n of 0.24 and 0.61 for upstream and downstream, respectively; Table S8 and Fig. 6). Doubled recharge (2R scenario) was the scenario that most consistently caused significant deviation from the baseline scenario (mean $D_n = 0.67$) in five out of six stream sites: Figs. 5 and 6). This might be explained by the significant impact of variation in groundwater recharge on hydraulic gradients which in turn affected the length of the streamlines and corresponding transit times in the unconfined aquifer system.

3.3. *Upstream particle tracking sites (6 km, 13 km, and 21 km)*

Groundwater discharge to streams was dominated by local shallow flow paths with short transit times in the upstream sites of 6 km, 13 km, and 21 km in each recharge and aquifer/riverbed scenario. The maximum MTT was around 7 years (Fig. S9 and Tables S3-S7). Observing shorter travel times at upstream particle tracking sites may be due to the partial penetration of the stream network in the headwaters of the watershed where intermediate and deeper flow paths did not converge into the stream cells. These cells act like weak sinks, permitting the underflow of groundwater beneath the river cells in the numerical

Table 2
Particle tracking simulations and related abbreviations used in the figures and text. Aquifer scenarios are increasing or decreasing vertically with increasing depth in the aquifer, while for Riverbed scenarios, parameter variation is from west to east.

Simulation Scenario		Abbreviation
Recharge	Uniform recharge, R = 55 mm yr^{-1}	uni
	Uniform recharge, 0.5R = 27.50 mm yr^{-1}	0.5R
	Uniform recharge, 0.75R = 41.25 mm yr^{-1}	0.75R
	Uniform recharge, 1.75R = 68.75 mm yr^{-1}	1.25R
	Uniform recharge, 2R = 110.00 mm yr^{-1}	2R
	Regional gradient – W to E increasing trend	rec_i
	Regional gradient – W to E decreasing trend	rec_d
	Lateral gradient	NDVI
	MODIS-estimated	MODIS
Aquifer	Increasing horizontal hydraulic conductivity	hc_i
	Decreasing horizontal hydraulic conductivity	hc_d
	Increasing vertical hydraulic conductivity	vc_i
	Decreasing vertical hydraulic conductivity	vc_d
	Increasing porosity	n_i
	Decreasing porosity	n_d
Riverbed	Longitudinal increase in riverbed conductivity	riv_i
	Longitudinal decrease in riverbed conductivity	riv_d
	Uniform riverbed conductivity, 0.05 m/d	riv_0.05
	Uniform riverbed conductivity, 5 m/d	riv_5
	Uniform riverbed conductivity, 50 m/d	riv_50

model (Abrams et al., 2012).

As explained below, TTDs for upstream sites are significantly different under riverbed hydraulic conductivity, doubled recharge, horizontal hydraulic conductivity, and porosity scenarios (Fig. 6 and Fig. S6). Especially under the lowest uniform riverbed hydraulic conductivity scenario (0.05 m/d), the TTD curves shifted towards older ages. For lower riverbed hydraulic conductivity, the connection between the aquifer and the stream is weakened (Lackey et al. 2015). This weakened connection results in variations in local hydraulic gradients, which in turn might affect the shorter flow paths discharging younger water at these sites (Goderniaux et al., 2013).

For constant aquifer thickness, an increase in recharge close to the outlet tends to generate much younger groundwater where the velocity is higher for the shorter flow paths close to the discharge point (Etcheverry, 2001; Leray et al., 2016; Leray et al., 2019). However, the doubled recharge (2R) scenario resulted in a shift towards larger transit times which is counterintuitive but can be explained by the large number of flooded cells (where simulated head is above the top of the cell) that altered the local flow paths and generated longer flow paths at the upstream of these stream sites (Fig. S10). This artificial condition occurs due to the unrealistic amount of recharge values, especially in the upstream part of the model domain, which acts as intermediate and regional recharge areas generating longer flow paths with larger transit times.

With the vertically increasing horizontal hydraulic conductivity scenario, where lower conductivities are in the upper model layers, the TTD curve was shifted to slightly older ages. This result is consistent with Etcheverry and Perrochet (2000) which found that when low hydraulic conductivity is in the upper model layers, the TTD shifts to older transit times because low hydraulic conductivity acts as a retardation factor. Similar decreases in transit times were reported in previous studies where hydraulic conductivities increased horizontally and/or vertically (Etcheverry and Perrochet 2000; Leray et al. 2019; Edington and Poeter 2006; Haitjema 1995). The porosity scenarios also have a strong effect on the transit times, where an increasing vertical trend (lower porosity in the upper layers) resulted in a shift towards younger ages in the upstream particle tracking sites. Effects of porosity can be explained by the higher flow velocities in the upper layers resulting in a shift to shorter transit times since the porosity is inversely proportional to the average linear groundwater velocity.

3.4. Intermediate particle tracking site (40 km)

The MTTs range from 10 years to 397 years in the 40 km site which is located just upstream of the confluence of the Upper, Middle and Northern branches of the UMLR. The TTDs were generally bimodal with very short (<1 year) and long transit times (e.g., uni, n_i, and 0.5R scenarios in Fig. 5; see also Fig. S9 and Tables S3-S7). Intermediate flow paths resulted in a spread in the TTDs and larger coefficient of variations in the MTTs were observed at this particle tracking site (Figures 6 and S9 and Tables S3 and S7). Unlike the upstream sites, the 40 km site yielded particles with older transit times which follow longer streamlines. The increasing horizontal hydraulic conductivity scenario resulted in a shift towards older ages as well as the highest KS-test score at this site. For geological settings where the hydraulic conductivity of the aquifer material increases with depth, Zlotnik et al. (2011) concluded that local and intermediate-depths flow systems disappear and/or are weakened and deeper groundwater circulation occurs where the water recharging the aquifer is pulled downward to the bottom portions of the flow domain. Riverbed hydraulic conductivity scenarios still had a large effect on the shape of the TTDs and the MTTs where a lower conductivity (0.05 md^{-1}) resulted in a shift towards older ages due to the reduced connection between the stream and aquifer. However, in contrast to the upstream study sites, the effect of doubled and halved recharge was greater at 40 km. The increasing porosity scenario (lower porosity in the upper layers) resulted in a shift towards shorter transit time and the shape of the TTD curve remained similar to the baseline scenario (Fig. 5). Overall, variations in the shape of the TTDs at this site might be related to spatial proximity to the middle branch of the UMLR and the local stream density which in turn affects the flow regime and the length of the particle streamlines discharging at this site.

3.5. Downstream particle tracking sites (99 km and 158 km)

In the downstream particle tracking sites (99 km and 158 km sites), recharge and aquifer scenarios significantly changed the shape of the TTD curves which were generally dominated by the particles traveling with intermediate and deep flow paths originating near the western, northern, and southern boundaries of the flow model. The simulated MTTs ranged from 820 to 2192 years and 2133 to 7968 years at 99 km and 158 km, respectively (Tables S3 and S9). The TTD curves generally had leptokurtic characteristics with long tails which is due to the fewer particles with longer streamlines and longer transit times (Fig. 5). The largest positive skewness (>1) was also observed in this particle tracking site. Doubled and halved recharge scenarios resulted in the most significant change in the TTDs and the MTTs at these sites (Fig. 6 and Fig. S8). Increased recharge (e.g., 2R scenario) scenario caused a shift towards shorter transit times while reducing the range of the transit times. This behavior in the TTD characteristics is parallel to the findings of previous modeling studies that assumed uniform aquifer thickness and recharge conditions (Haitjema, 1995; Etcheverry, 2001; Leray et al., 2016; Leray et al., 2019). The overall behavior of increasing MTT with decreased recharge rate (Fig. 7) was also consistent with lumped-parameter models (e.g., exponential model, Vogel 1967, Solomon et al., 2006). Halved recharge (0.5R), on the other hand, resulted in a shift towards older ages due to weakening of local flow paths close to the particle tracking sites as well as the slower input to a certain volume caused a longer residence time. Engdahl and Maxwell (2015) also obtained a similar TTD shift to older ages when they decreased the recharge by 50 % in their numerical groundwater model. Additionally, under low recharge conditions, the TTD curve shifts to longer transit times with decreasing level of stream and aquifer interaction (due to the weakening of local flow paths) (Goderniaux et al., 2013). The downstream transects were also affected less by the flooded and dried model cells in the upstream part of the model domain under 0.5R and 2R

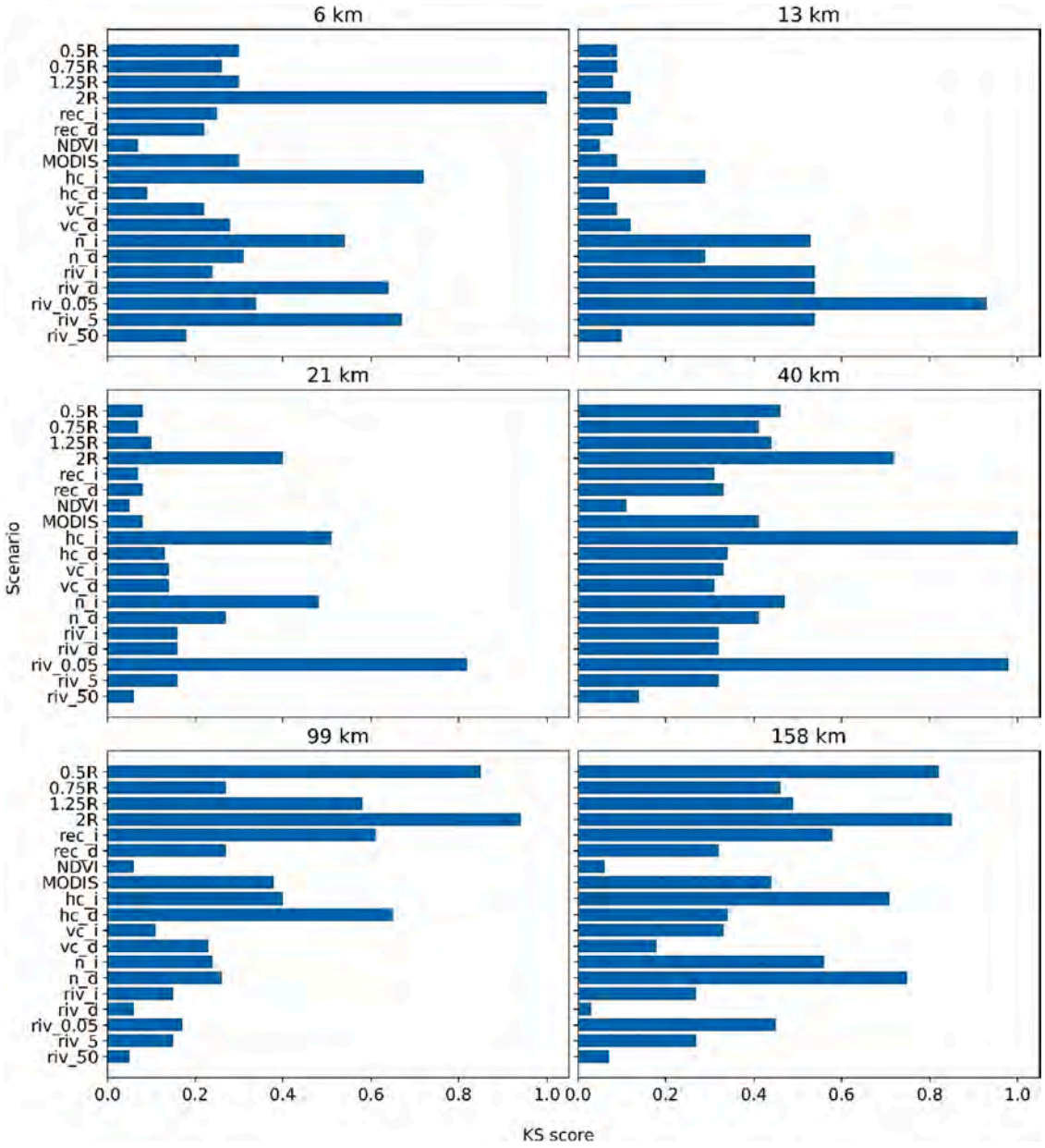

Fig. 6. Kolmogorov-Smirnov (KS) test scores based on the baseline scenario at six different locations in the stream (Fig. 2). Refer to Table 2 for information on scenario names.

recharge scenarios.

Unlike at the upstream sites, riverbed conductivity scenarios had less impact on the TTDs at 99 km and 158 km (Fig. 8). The TTDs were more sensitive to a variation in aquifer hydraulic conductivity than the riverbed conductivity in these downstream particle tracking sites (Figs. 5 and 6). Similarly, Kalbus et al. (2009) reported that the aquifer heterogeneity plays a more important role than the riverbed heterogeneity in groundwater discharge to streams. Overall, shapes of the TTD curves (Fig. 6) are closer to an exponential distribution moving from 99 km to 158 km (i.e., as spatial scale increased) where the discharge point is closer to the outlet of the ground watershed under a uniform recharge, as discussed in Haitjema (1995).

4. Implications and future work

In this study, the steady-state 3D groundwater flow model utilized an actual catchment geometry together with hypothetical recharge, aquifer, and riverbed parameter scenarios. The particle tracking was based on the advective transport of groundwater parcels in the flow domain. Simulations indicate significant change in the transit times in most of the simulation scenarios. This 'age' shift from the baseline scenario was also more prominent in the TTDs than in the MTTs (e.g., Fig. 6 and Fig. S8).

The results of the particle tracking simulations also showed that the transit times were not only controlled by different model parameters such as recharge or aquifer's hydraulic parameters but also the local- and regional-scale groundwater conditions at different particle tracking sites. For example, the upstream discharge sites were dominated by local and shallow flow system in which the effects of disconnection between aquifer and stream (e.g., a very low riverbed conductivity scenario) was more significant due to the disappearing of local hydraulic gradients at these stream sites. However, in the downstream sites, groundwater discharge is mainly dominated by intermediate and deeper flow systems and affected less by the riverbed conductivity since the regional

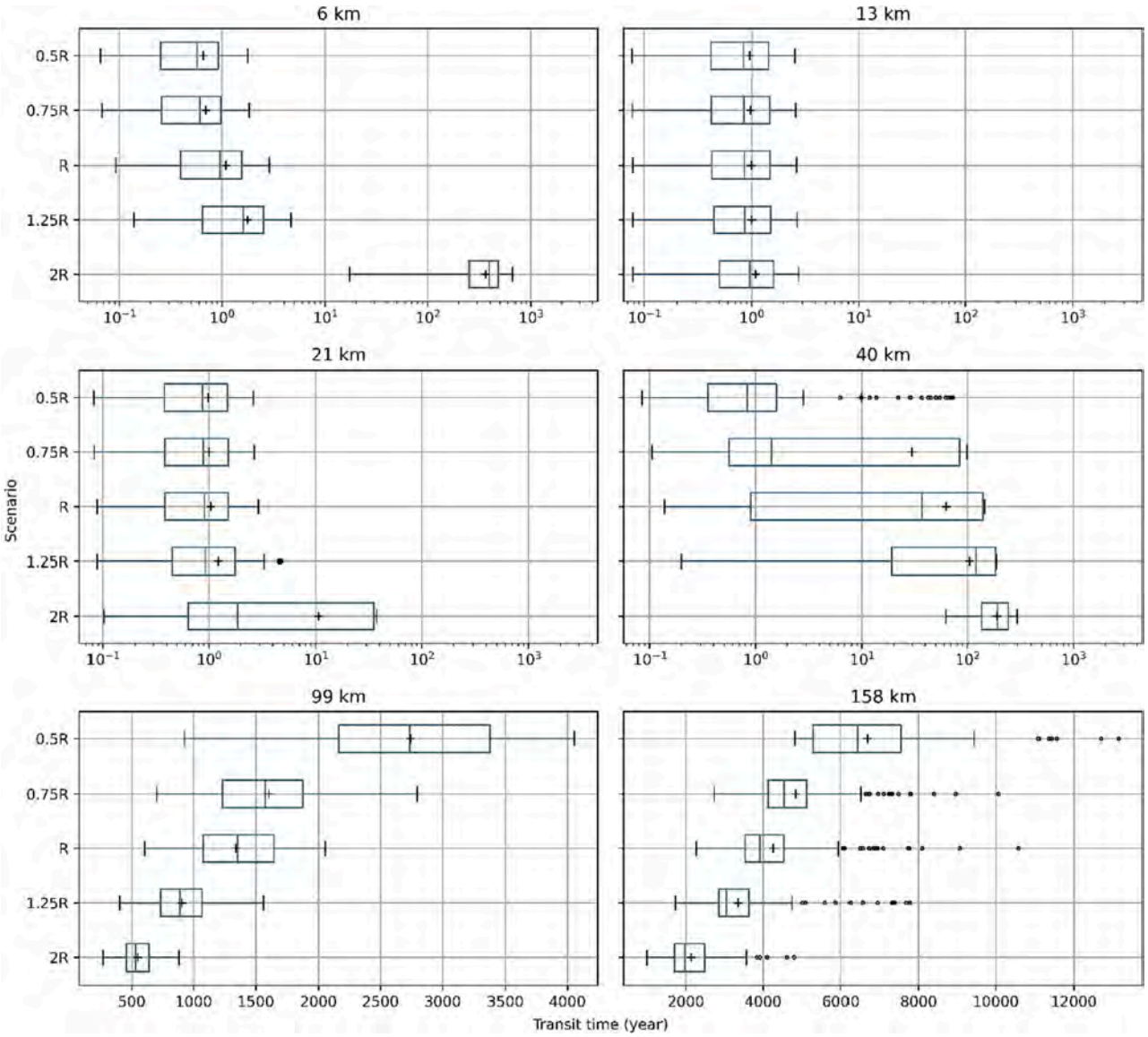

Fig. 7. Boxplots of travel times at six particle tracking sites in the stream (Fig. 2) under varying uniform recharge values (means and outliers are shown with + and circles, respectively). Each scenario had 1800 unique particles.

groundwater flow direction and the longer streamlines were not significantly affected. The KS test scores (Fig. 6 and Fig. S8) also suggest that the TTDs at the study sites were less sensitive to spatially varying recharge scenarios (e.g., MODIS-estimated or lateral recharge gradient scenario) than a uniform change in the magnitude of recharge (e.g., halved or doubled recharge).

Outliers in transit times were generally observed at sites 40 km and 158 km (Fig. S9). It can be explained by very short and very long streamlines modeled based on the groundwater velocity distributions and the particle tracking algorithm that allows a particle to terminate within a boundary cell in the model domain. This makes a small number of particles terminate faster or slower than most of the particles. For example, at 158 km, some of the particles are traveling with very long regional flow paths without being terminated at a boundary cell thus reaching at the very eastern part of the model domain (Fig. 4).

For any hydrological model, uncertainty exists in each input yet there are finite resources available for data collection. Though the sensitivity of model parameters in other study sites may not have the same results as ours, the results of this study can help guide future modeling TTD studies in the identification of the most influential model parameters. This information can help them prioritize their data collection efforts. Overall, the results indicate that the sensitivity of the model parameterization on the TTDs should also be investigated by considering the spatial characteristics of the regional aquifer system. This emphasizes the importance of using local calibration targets such as groundwater tracer ages in the numerical model calibration process. Considering the actual geological heterogeneity of the aquifer system by using a 3D model will also improve the accuracy of the particle streamlines and related TTD predictions. The TTDs also were affected by the accuracy of the particle tracking of the coarse numerical model grids (>125 m) that do not represent the actual stream area or geometry in the watersheds (Abrams, 2013). This regional scale grid discretization also limited the understanding of the link between the topography and dynamics of groundwater flow movement/TTDs due to the hummocky topography in the NSH. The local grid refinement and/or small-scale numerical model development, especially, in the target sites (e.g., particle tracking/groundwater sampling sites) may eventually increase the accuracy of the predictions of the future numerical models.

This study was an important step toward understanding the potential hydrological mechanisms driving discrepancies between the TTDs obtained from numerical model and groundwater age-dating tracer studies in the UMLR watershed. In future research, comparison of calibrated

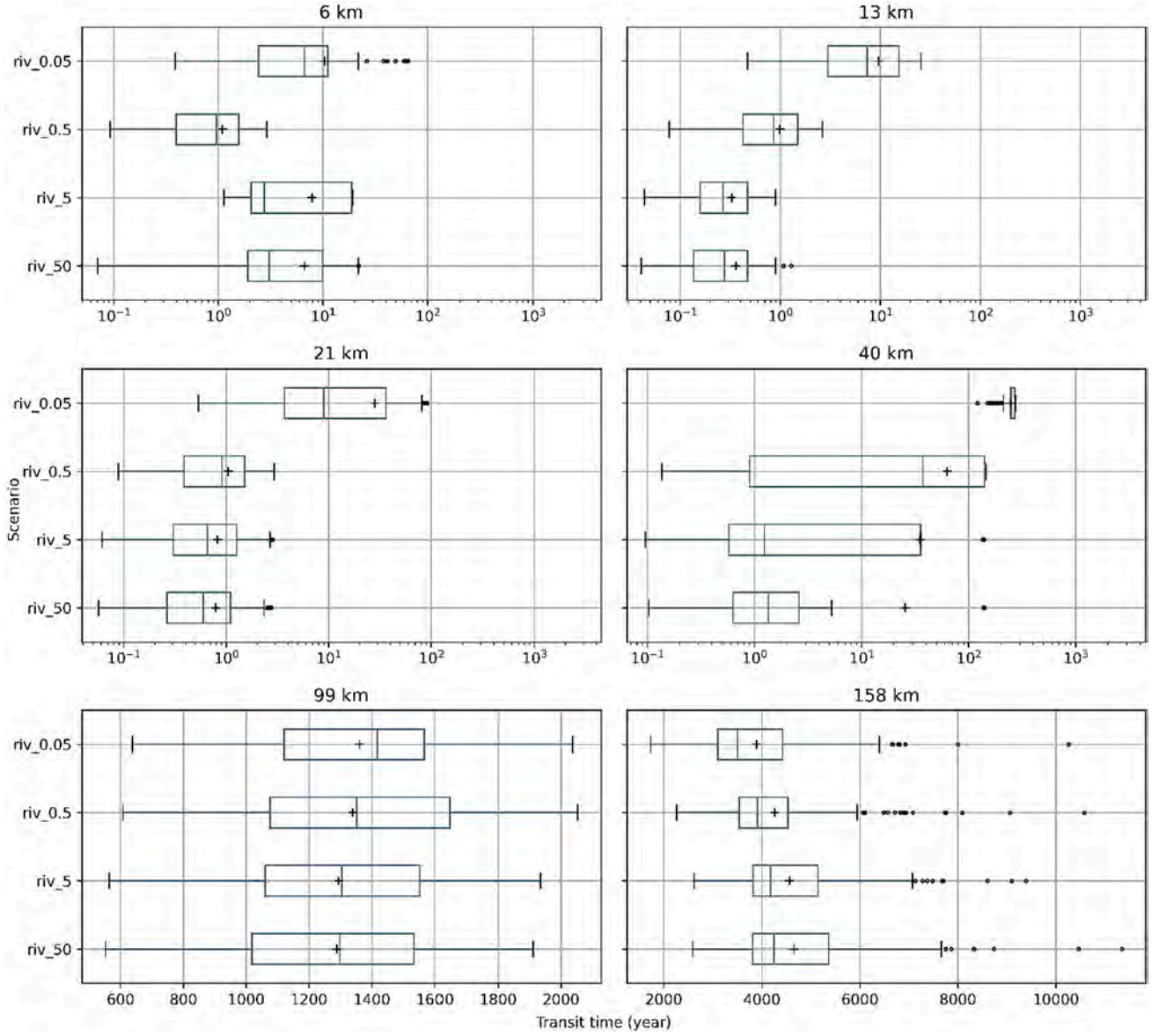

Fig. 8. Boxplots of travel times at six particle tracking sites in the river (Fig. 2) under varying uniform riverbed hydraulic conductivity scenarios (means and outliers are shown with + and circles, respectively). Each scenario had 1800 unique particles.

model TTDs and age-dating tracer TTDs can refine the understanding of the hydrological processes and discrepancies between the different estimation methods. Collectively, these studies will provide guidance for future particle tracking simulations, both for incorporating environmental tracer information into groundwater model calibration and for using particle tracking as a preliminary guide when designing field tracer studies.

5. Conclusions

The TTDs of groundwater discharges at six different river sites in the UMLR watershed were modeled using coupled numerical groundwater flow modeling (MODFLOW-USG) and particle tracking (MODPATH 3DU) under varying recharge, aquifer, and riverbed heterogeneity scenarios. Obtained MTTs and TTDs were compared with a baseline scenario, using the real aquifer geometry, and represented with five vertical layers with uniform recharge, aquifer, and stream parameters.

Simulation results showed how the MTTs and TTDs spatially vary in response to these parameter scenarios with a clear upstream to downstream increasing trend in the UMLR watershed (maximum MTTs range between 7 years and 7968 years). Upstream particle tracking sites were characterized with local and shallow flow paths with short transit times while downstream sites were dominated by intermediate and deeper flow paths with significantly longer transit times. Furthermore, the effect of each scenario on TTDs and MTTs also varied at each particle tracking site. In the upstream particles tracking sites, transit times were generally more sensitive to a change in riverbed hydraulic conductivity while increasing and decreasing uniform recharge had more control on the shape of the TTDs in the downstream sites in the flow domain. Results showed that the different model parameters were important for controlling the TTDs for different parts of the watershed, where the particle travel paths vary depending on the conditions of local and regional groundwater system across the recharge and discharge zones.

Declaration of Competing Interest

The authors declare that they have no known competing financial interests or personal relationships that could have appeared to influence the work reported in this paper.

Data availability

Data will be made available on request.

Acknowledgements

This material is based upon work supported by the National Science Foundation under Grant No. 1744719, 1744714, and 1744721. The authors thank Dr. Sorab Panday for the constructive comments and suggestions on the numerical model. We also acknowledge United States Department of Agriculture National Institute of Food and Agriculture, Hatch project NEB-21-177 (accession number 1015698; T. Gilmore and A. Mittelstet) and graduate student support from the Daugherty Global Water for Food Institute at the University of Nebraska.

Appendix A. Supplementary data

Supplementary data to this article can be found online at https://doi.org/10.1016/j.jhydrol.2022.128891.

References

Abrams, D., Haitjema, H., Kauffmann, L., 2012. On Modeling Weak Sinks in MODPATH. Groundwater.

Abrams, D., Haitjema, H.M., 2018. H. How Aquifer Characteristics of a Watershed Affect Transit Time Distributions of Groundwater. Ground Water 56(4), 517–520. https://doi.org/10.1111/gwat.12788.

Anderson, M.P., Woessner, W.W., Hunt, R.J., 2015. Applied groundwater modeling: Simulation of flow and advective transport. Academic Press, p. 564.

Basu, N.B., Jindal, P., Schilling, K.E., Wolter, C.F., Takle, E.S., 2012. Evaluation of analytical and numerical approaches for the estimation of groundwater travel time distribution. Journal of Hydrology 475, 65–73.

Browne, B.A., Guldan, N.M., 2005. Understanding Long-Term Baseflow Water Quality Trends Using a Synoptic Survey of the Ground Water-Surface Water Interface, Central Wisconsin. Journal of Environmental Quality 34, 825–835.

Cardenas, M.B., Jiang, X.-W., 2010. Groundwater flow, transport, and residence times through topography-driven basins with exponentially decreasing permeability and porosity. Water Resour. Res. 46, W11538.

Chakravarti, I., M., Laha, R., and G., Roy J., (1967). "Handbook of Methods of Applied Statistics, Volume I," John Wiley and Sons, Hoboken, pp. 392-394.

Conservation and Survey Division of University of Nebraska-Lincoln (2019). Configuration of the Base of the Principal Aquifer, 1979, accessed December 29, 2019 at https://snr.unl.edu/data/geographygis/water.aspx.

Conservation and Survey Division of University of Nebraska-Lincoln (2019). 1995 Water Table Contour for the state of Nebraska, accessed December 29, 2019 at http://cohyst.nebraska.gov/archive/cohyst_preliminarydata.html.

Craig, J.R., Ramadhan, M., Muffels, C., 2020. A particle tracking algorithm for arbitrary unstructured grids. Groundwater 58 (1), 19–26.

Dappen, P., Merchant, J., Ratcliffe, I., Robbins, C., 2007. Delineation of 2005 land use patterns for the state of Nebraska Department of Natural Resources, Final Rep. In: Center for Advanced Land Management Information Technologies. University of Nebraska-Lincoln, Lincoln, Nebraska, p. 80 p..

Deering, D. W. (1978). Rangeland reflectance characteristics measured by aircraft and spacecraft sensor. Texas A&M University.

Dietze, M., Dietrich, P., 2012. Evaluation of vertical variations in hydraulic conductivity in unconsolidated sediments. Groundwater 50 (3), 450–456.

Domenico, P.A., Schwartz, F.W., 1990. Physical and Chemical Hydrogeology. John Wiley and Sons, New York, p. 824.

Earnest, E., Boutt, D., 2014. Investigating the role of hydromechanical coupling on flow and transport in shallow fractured-rock aquifers. Hydrogeol. J. 22 (7), 1573–1591.

Edington, D., Poeter, E., 2006. Stratigraphic control of flow and transport characteristics. Ground Water 44, 826–831.

Engdahl, N.B., Maxwell, R.M., 2015. Quantifying changes in age distributions and the hydrologic balance of a high-mountain watershed resulting from climate induced variations in recharge. Journal of Hydrology 522, 152–162. https://doi.org/10.1016/j.jhydrol.2014.12.032.

Etcheverry, D., Perrochet, P., 2000. Direct simulation of groundwater transit-time distributions using the reservoir theory. Hydrogeology Journal 8 (2), 200–208.

Fetter, C.W. (2001). Applied Hydrogeology. 4th Edition, Prentice Hall, Upper Saddle River, 2, 8.

U.S. Geological Survey, 2017, 1/3rd arc-second Digital Elevation Models (DEMs) - USGS National Map 3DEP Downloadable Data Collection: U.S. Geological Survey.

U.S. Geological Survey (2022). Elevation Source Data (3DEP) - Lidar, IfSAR, accessed April 29, 2021 at https://apps.nationalmap.gov/downloader.

Gilmore, T.E., Genereux, D.P., Solomon, D.K., Solder, J.E. (2016). Groundwater transit time distribution and mean from streambed sampling in an agricultural coastal plain watershed, North Carolina, USA Water Resour. Res.

Goderniaux, P., Davy, P., Bresciani, E., de Dreuzy, J.-R., Le Borgne, T., 2013. Partitioning a regional groundwater flow system into shallow local and deep regional flow compartments: groundwater partitioning. Water Resour. Res. 49, 2274–2286.

Goode, J.D., 1996. Direct Simulation of Groundwater age, Water Resour. Res. 32, 289–296.

Gudmundsen Sandhills Laboratory | Nebraska Extension [WWW Document], n.d. URL https://extension.unl.edu/statewide/westcentral/gudmundsen-sandhills-laboratory/(accessed 2.9.22).

Gutentag, E.D., Heimes, F.J., Krothe, N.C., Luckey, R.R., and Weeks, J.B., (1984). Geohydrology of the High Plains aquifer in parts of Colorado, Kansas, Nebraska, New Mexico, Oklahoma, South Dakota, Texas, and Wyoming: U.S. Geological Survey Professional Paper 1400–B, 63 p.

Harbaugh, A.W., (2005). MODFLOW-2005, the U.S. Geological Survey modular ground-water model - The ground-water flow process: U.S. Geological Survey Techniques and Methods 6–A16, variously paged. http://pubs.er.usgs.gov/publication/tm6A16.

Hobza, C.M., and Schepers, A.R., (2018). Groundwater discharge characteristics for selected streams within the Loup River Basin, Nebraska, 2014–16: U.S. Geological Survey Scientific Investigations Report 2018–5093, 50 p., 10.3133/sir20185093.

Houston, N.A., Gonzales-Bradford, S.L., Flynn, A.T., Qi, S.L., Peterson, S.M., Stanton, J. S., Ryter, D.W., Sohl, T.L., and Senay, G.B., (2013). Geodatabase compilation of hydrogeologic, remote sensing, and water-budget-component data for the High Plains aquifer, 2011: U.S. Geological Survey Data Series 777, 12 p., accessed March 7, 2017.

Humphrey, E., D.K. Solomon, T.E. Gilmore, A.R. Mittelstet, V.A. Zlotnik, D.P. Genereux, C. Zeyrek, M.R. MacNamara, and C.R. Jensen (2020). Using empirical transit time distributions to forecast stream water tracer concentrations. AGU Fall Meeting, Virtual. December 1-17, 2020. Poster presentation. https://agu.confex.com/agu/fm20/meetingapp.cgi/Paper/666576.

Haitjema, H.M., 1995. On the residence time distribution in idealized groundwatersheds. J. Hydrol. 172 (1–4), 127–146.

Ilampooranan, I., Van Meter, K.J., Basu, N.B., 2019. A race against time: Modeling time lags in watershed response. Water Resources Research 55, 3941–3959. https://doi.org/10.1029/2018WR023815.

Irvine, D.J., Brunner, P., Franssen, H.-J.-H., Simmons, C.T., 2012. Heterogeneous or homogeneous? Implications of simplifying heterogeneous streambeds in models of losing streams. J. Hydrol. 424, 16–23.

Jing, M., Heße, F., Kumar, R., Kolditz, O., Kalbacher, T., Attinger, S., 2019. Influence of input and parameter uncertainty on the prediction of catchment-scale groundwater travel time distributions Hydrol. Earth Syst. Sci. 23 (2019), 171–190. https://doi.org/10.5194/hess-23-171-2019.

Kalbus, E., Schmidt, C., Molson, J.W., Reinstorf, F., Schirmer, M., 2009. Influence of aquifer and streambed heterogeneity on the distribution of groundwater discharge. Hydrol. Earth Syst. Sci. 13, 69–77. https://doi.org/10.5194/hess-13-69-2009.

Kennedy, C.D., Genereux, D.P., Corbett, D.R., Mitasova, H., 2009. Relationships among groundwater age, denitrification, and the coupled groundwater and nitrogen fluxes through a streambed. Water Resources Research 45 (9).

Korus, J.T., Burbach, M.E., Howard, L.M., Joeckel, R.M., 2011. Nebraska statewide groundwater-level monitoring report 2010, Nebraska Water Survey Paper 77. Conservation and Survey Division, University of Nebraska-Lincoln, p. 19.

Kurtz, W., Hendricks Franssen, H.-J., Brunner, P., Vereecken, H., 2013. Is high resolution inverse characterization of heterogeneous river bed hydraulic conductivities needed and possible? Hydrol. Earth Syst. Sci. 17 (10), 3795–3813.

Leray, S., Gauvain, A., de Dreuzy, J.R., 2019. Residence time distributions in non-uniform aquifer recharge and thickness conditions. An analytical approach based on the assumption of Dupuit-Forchheimer. J. Hydrol. 574, 110–128.

Loope, D., Swinehart, J. (2000). Thinking Like a Dune Field: Geologic History in the Nebraska Sand Hills. Gt. Plains Res. A J. Nat. Soc. Sci.

Maloszewski, P., 2000. Lumped-Parameter Models as a Tool for Determining the Hydrological Parameters of Some Groundwater Systems Based on Isotope Data 262. IAHS-AISH Publication, pp. 271–276.

Małoszewski, P., Zuber, A., 1982. Determining the turnover time of groundwater systems with the aid of environmental tracers 1. Models and their applicability. J. Hydrol. 57, 207–231. https://doi.org/10.1016/0022-1694(82)90147-0.

Maxwell, R.M., Condon, L.E., Kollet, S.J., Maher, K., Haggerty, R., Forrester, M.M., 2016. The imprint of climate and geology on the residence times of groundwater. Geophysical Research Letters 43 (2), 701–708.

Modica, E., Buxton, H.T., Plummer, L.N., 1998. Evaluating the source and residence times of groundwater seepage to streams, New Jersey Coastal Plain. Water Resources Research 34 (11), 2797–2810.

Muffels, C., Tonkin, M., Ramadhan, M., Wang, X., Neville, C., Craig, J.R., 2016. User's Guide for Modpath3DU. A groundwater path and travel-time simulator. S.S., University of Waterloo.

Myneni, R.B., Hall, F.G., Sellers, P.J., Marshak, A.L., 1995. The interpretation of spectral vegetation indexes. IEEE Trans. Geosci. Remote Sens. 33, 481–486. https://doi.org/10.1109/tgrs.1995.8746029.

Naumburg, E., Mata-gonzalez, R., Hunter, R., Mclendon, T., Martin, D., 2005. Phreatophytic Vegetation and Groundwater Fluctuations: A Review of Current Research and Application of Ecosystem Response Modeling with an Emphasis on Great Basin Vegetation. Environmental Management 35 (6), 726–740.

Panday, S., Langevin, C.D., Niswonger, R.G., Ibaraki, M., Hughes, J.D., 2013. MODFLOWUSG version 1: An unstructured gird version of MODFLOW for simulating groundwater flow and tightly coupled processes using a control volume finite difference formulation: U.S. Geological Survey Techniques and Methods 6 A45.

Parizi, E., Hosseini, S.M., Ataie-Ashtiani, B., 2020. Normalized difference vegetation index as the dominant predicting factor of groundwater recharge in phreatic

aquifers: case studies across Iran. Sci Rep 10, 17473. https://doi.org/10.1038/s41598-020-74561-4.
Rossman, N.R., Zlotnik, V.A., Rowe, C.M., 2018. An approach to hydrogeological modeling of a large system of groundwater-fed lakes and wetlands in the Nebraska Sand Hills, USA. Hydrogeology Journal 26 (3), 881–897.
Rumbaugh, J.O., and D.B. Rumbaugh, Groundwater Vistas Version 7 (2017). Environmental Simulations Inc. (ESI), Leesport PA.
Rumynin, V.G., Leskova, P.G., Sindalovskiy, L.N., Nikulenkov, A.M., 2019. Effect of depth-dependent hydraulic conductivity and anisotropy on transit time distributions. Journal of Hydrology 579.
Sanford, W.E., 2011. Calibration of models using groundwater age. Hydrogeol. J. 19, 1–4.
Schmeisser McKean, R.L., Goble, R.J., Mason, J.B., Swinehart, J.B., Loope, D.B., 2015. Temporal and spatial variability in dune reactivation across the Nebraska Sand Hills, USA. The Holocene 25 (3), 523–535. https://doi.org/10.1177/0959683614561889.
Seeyan, S., Merkel, B., Abo, R., 2014. Investigation of the relationship between groundwater level fluctuation and vegetation cover by using NDVI for Shaqlawa Basin, Kurdistan Region-Iraq. J. Geogr. Geol. 6, 187–202.
Solomon, D.K., Cook, P.G., Plummer, L.N., 2006. Models of groundwater ages and residence times. In: Use of ChlorofluorocArbons in Hydrology: A Guidebook. Int. Atomic Energy Agency, Vienna, Austria, pp. 73–88.
Szilagyi, J., Harvey, E.F., Ayers, J., 2003. Regional estimation of base recharge to ground water using water balance and a base-flow index. Ground Water 41 (4), 504–513.
Szilagyi, J., Jozsa, J., 2013. MODIS-Aided Statewide Net Groundwater-Recharge Estimation in Nebraska. Groundwater 51 (5), 735–744. https://doi.org/10.1111/j.1745-6584.2012.01019.x.
Szilagyi, J., Zlotnik, V.A., Gates, J.B., 2011. Mapping mean annual groundwater recharge in the Nebraska Sand Hills, USA. Hydrogeol J 19, 1503–1513.
Tang, Q., Kurtz, W., Schilling, O.S., Brunner, P., Vereecken, H., Franssen, H.H.J., 2017. The influence of riverbed heterogeneity patterns on river-aquifer exchange fluxes under different connection regimes. J. Hydrol. 554, 383–396.
Todd, D., Mays, L., 2005. Groundwater Hydrology, 3rd ed. John Wiley and Sons Inc, Hoboken, p. 652.
Varni, M., Carrera, J., 1998. Simulation of groundwater age distribution. Wat Resour Res 34 (12), 3271–3281.
Vermote, E., Justice, C., Claverie, M., Franch, B., 2016. Preliminary analysis of the performance of the Landsat 8/OLI land surface reflectance product. Remote Sens. Environ. 185, 46–56. https://doi.org/10.1016/j.rse.2016.04.008.
Vogel, J.C., 1967. Investigation of groundwater flow with radiocarbon. In Isotopes in Hydrology, Proceedings, IAEA, Vienna 1967, 355–369.
Wang, P., Zhang, Y., Yu, J., Fu, G., Ao, F., 2011. Vegetation dynamics induced by groundwater fluctuations in the lower Heihe River Basin, northwestern China. Journal of Plant Ecology 4 (1–2), 77–90.
Zlotnik, V.A., Cardenas, M.B., Toundykov, D., 2011. Effects of multiscale Anisotropy on Basin and Hyporheic Groundwater Flow. Groundwater 49 (4), 576–583.

Further reading

Haitjema, H.M., 1995a. Analytic Element Modeling of Groundwater Flow. Academic Press Inc., San Diego, California.
Haitjema, H.M., 1995b. On the residence time distribution in idealized groundwatersheds. J. Hydrol. 172 (1–4), 127–146.